ISSN: 2639-7536

Research Article

Petroleum and Chemical Industry International

Effect of C oncentration of Mo on the Mechanical behavior of γ UMo: an Atomistic Study

Asmat Ullah[1*], Wang Qingyu[1], Muhammad Ado[1], M Mustafa Azeem[2], Ahmer Shah[3]

[1]*College of Nuclear Science and Technology, Harbin Engineering University, Harbin, 150000, China.*

[2]*School of Nuclear Science and Technology, Xian Jiaotong University, Xian, China.*

[3]*Department of Material Science, Balochistan University of Information Technology, Management and Engineering Sciences, Quetta, China.*

[*]Corresponding author
Asmat Ullah, College of Nuclear Science and Technology, Harbin Engineering University, Harbin, 150000, China.

Submitted: 15 Dec 2021; **Accepted**: 21 Dec 2021; **Published**: 30 Dec 2021

Citation: *Asmat Ullah., Wang Qingyu., Muhammad Ado., M Mustafa Azeem., Ahmer Shah. (2021). Effect of concentration of Mo on the mechanical behavior of γ UMo: An atomistic study. Petro Chem Indus Intern, 4(3), 67-71*

Abstract

We performed molecular dynamics simulation on nanoindentation ofγ phase Uranium Molybdenum alloys using spherical indenter. A ternary potential developed for UMoXe was utilized. We calculated the updated values for hardness and reduced elastic modulus at different concentrations of Mo. The whole process of deformation and dislocation analysis was visualized using OVITO. We found an increase in deformation withincreasein stress while dislocations are not found anyhow induced defects have been distributed throughout the simulation cell randomly. The increase in concentration affected the hardness and reduced elastic modulus significantly. This study provides insights into the structure and mechanical characteristics of γ UMo under deformation.

Keywords: Nanoindentation, MD Simulation, UMo Fuel, Spherical indenter

Introduction

The element uranium is an actinide exhibiting delocalized f electrons,exists in three solid allotropic forms: α(face-centered orthorhombic), β(body-centered tetragonal) and γ(body-centered cubic)[1]. At high temperatures, uranium transforms from αto βat approximately 935 K and β transforms to γ at approximately1045 K [2]. Several transition metals, particularly 4d and 5d elements in Group IV, through VIII, form solid solutions with γ-U, and this cubic phase can be retained in its metastable state upon cooling. It was early recognized that Mo, which has substantial solubility in U (~35%) presents a good compromise between the amount needed to stabilize γ-U and acceptable U density so achieved [3, 4]. Low Enriched Uranium (LEU) fuels play an indispensable role in peaceful purposes of nuclear energy. γUranium Molybdenum (UMo) is a LEU alloy which is considering an attractive fuel for fast and pressurized water reactors. It is ease in fabrication with inviting characteristics such as high thermal conductivity, good structural stability and reliable mechanical strength [5, 6]. Understanding the integrity during operations whether normal or transient or anticipated faults is of high importance for the better functionality of a nuclear fuel. The fission products are only released from a fuel plate during irradiation if a defect exists in the cladding that provides a path for fission gas to escape [7]. These defects under stress and temperature fields eventually lead to swelling or pores which ultimately either limit the performance or permanent failure of the fuel [8]. A group of researchers on experimental basis showed that the brittleness and fracture aredependent on Mo concentration [9]. In this work we performed a number of MD simulationsusing LAMMPS code to investigate the impact on the nanomechanical properties of variable Mo concentration in γUMo.A spherical indenter of defined radius was used and its depth with varying load was analyzed.Dislocations creation, grain formation and segregation were tracked using OVITO.

Method

MD simulations were performedusing Large scale Atomic/ Molecular Massively Parallel Simulator (LAMMPS) [10]. The EAMpotential developed by Smirnova [11] is used in this work. Periodic boundary conditions were applied in the x and y while shrink style was used along the z axis. A simulation cell of 129600 atoms was created. The relaxation was conducted using the NVT ensemble at 300 K using the velocity Verlet algorithm at 300 K with a time step of 1 fs for 100,000 steps. The system was relaxed again at 100 ps for the same number of steps using NVE ensemble [12].Using Langevin's thermostat [13] we kept the temperature constant at 300 K. A rigid spherical indenter was used with radius of 35 A0, and the impact of force on each atom was tracked. A non atomic repulsive sphere exerts a force on the atomic layer which

can be quantified using equation (1)

$$F = -K\,(r - R)^2 \qquad (1)$$

where R is the radius of the indenter and r is the distance from the atom to the center of the indenter. The speed of the indenter during loading and unloading was 0.1 Å/ps which will penetrate it to a maximum depth of 20 Å. We conducted simulations for four different concentrations of Mo in the alloy. The atomistic events at different input conditions were analyzed and visualized via Open Visualizations Tool (OVITO) [14].

$$U = \sum_{i<j} \varphi_{\alpha\beta}(r_{ij}) + \sum_{j} F_{\alpha}(\rho_j), \quad \rho_j = \sum_{j \neq i} \rho(r_{ij}) \qquad (2)$$

$$\alpha, \beta = U, MO, Xe$$

Interatomic potential

An interatomic potential for UMo system with Xe is developed within the framework of an embedded atom model using a force matching technique and a dataset of ab initioatomic forces. The verification of potential proves that it is suitable for investigation of various compounds existing in the system as well as for simulation of pure elements: U, Mo and Xe. The obtained values for lattice constants, thermal expansion coefficients, melting temperatures, elastic properties and formation energies are consistent with the experimental and ab-initiocalculations. The development of this potential has been performed within the framework of the embedded atom method (EAM) which considers the many particle interactions. This model has shown to be convenient in the cases of binary systems and pure Usystems [15, 16].The potential of the system can be represented mathematically as

where pair potential is $\varphi_{\alpha\beta}$ and r_{ij} is the interatomic distance between any two given atoms. α,β=U,MO,Xe and ρ_i is an effective electron density. At a given cut off radius both the functions ρ and φ fall to zero. The function F_α in the second term is standing for many body effects and is a non linear embedding function.

Results

Nanoindentation is generally the most common technique to study nanomechanical qualities properties of a sample. In this process we made use of substrate to hold the target at a fixed position so it may prevent atoms from shifting during indentation. The schematic representation of nanoindentation using a spherical indenter is shown in figure 1.

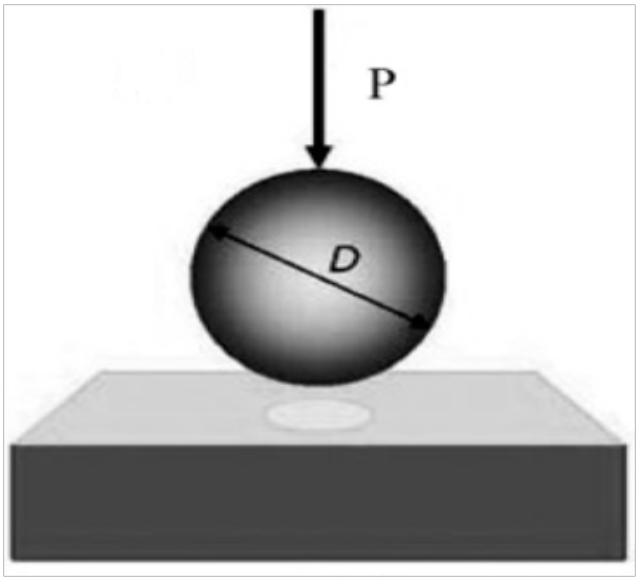

Figure:1 Schematic diagram of nanoindentation using spherical indenter

The change in grain boundaries with the application of load were visualized with OVITO at different intervals of time and the residual impact of the spherical indenter on the surface of the target has been shown in the figure 2.

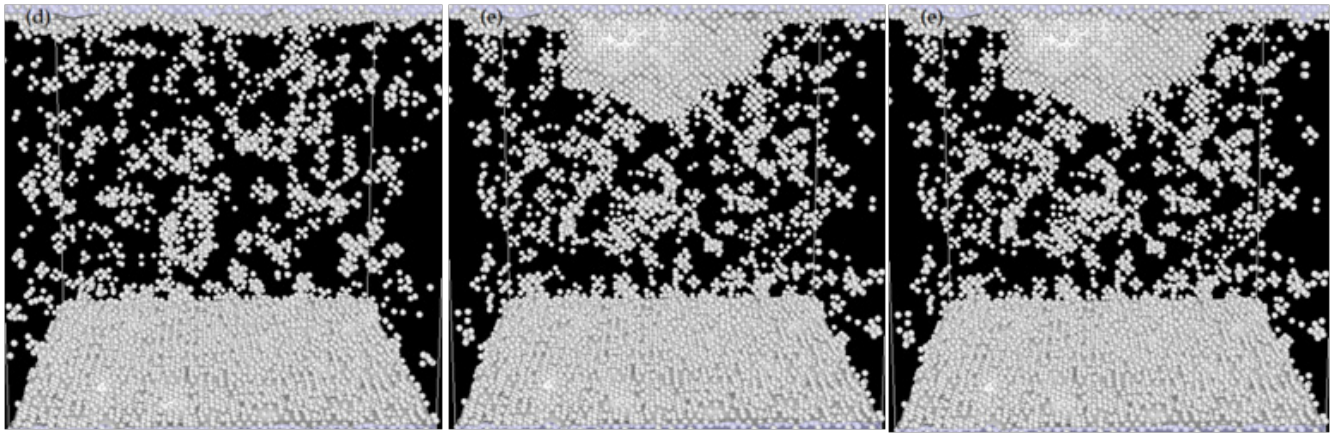

Figure: 2: From (a)-(c) shows the deformation mechanism along with grain segmentation while (e)-(f) show the DXA analysis at different time intervals.

The maximum value of the penetration depth of the sample into the sample was recorded 20 A0. In figure 2 from (a)-(c) is showing the grains which were under the application of external load showed variation in size.During analysis it was observed that the impact of applied stress is not producing any permanent dislocations but the defects induced due to applied stress are scattered randomly. At different timescales we have identified the penetration depth of the indenter by slicing the simulation cell in OVITO. We conducted the dislocation analysis by involving the Dislocation Analysis (DXA) identifier and the results at different simulation times are presented in figure.2 from (e) to (f). Just like in ceramics nonexistence of dislocations has been found in UMo alloy at all the said concentrations of Mo[17].

In the qualities study of nanoindentation the loading part is assumed to be the plastic while the unloading curve is representing the elastic regime. Figure.3 tells us that just like all the metal the target of UMo is also hardening as the load is increasing with the depth.

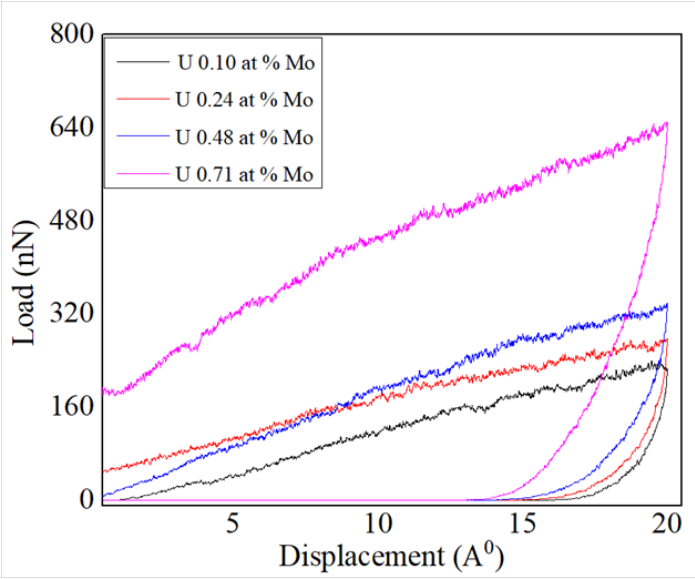

Figure 3: Loading-unloading processes during nanoindentation

No significant pop in were observed. The absence of dislocations and these pop in the process record no plastic events. We observed that increase in the density of Mo required higher load to penetrate to the same depth and significant increase is measured with 0.71 at % Mo.

Hardness is the resistance to local deformation such as indentation, scratches or plastic deformation. Mathematically the hardness is given by

$$H = \frac{P_{max}}{A_c} \tag{3}$$

where P_{max} is representing the maximum value of the force applied by the indenter and Ac is the residual contact area which is given by $A_c = \pi R h_c$ where

$$h_c = h_{max} - \frac{P_{max}}{S_{max}}$$

In order to predict the strength of resistance to deformation at different levels of Mo concentration we worked on the reduced elastic modulus which can be obtained from the unloading data and is mathematically given by

$$E_r = \frac{1}{2\beta}\frac{\sqrt{\pi}}{A_c}\frac{dp}{dh} \tag{4}$$

where β is a constant carrying information about shape of the indenter and its value for spherical indenter is 1.034. Er is equivalent reduced elastic modulus and *dp/dh* is the stiffness which can be obtained from the initial part of unloading curve. In order to fit the function at the maximum indenter's displacement, the initial process of unloading can be regarded as elastic deformation. Therefore, we choose different intervals in the unloading process for linear fitting and found out the mean value. Unloading part of the P-h curve is usually fitted using the following function,

$$P = \alpha(h - h_f)^m \tag{5}$$

and

$$S = \left(\frac{dp}{dh}\right)_{h=h_{max}} = \alpha m(h_{max} - h_r)^{m-1} \tag{6}$$

h_{max} is the maximum indentation depth [20] and h_r is the residual depth after unloading wherebyα and m are constants with values 1.5 for each in case of a spherical indenter [18]. The slope of each unloading curve is obtained for calculating the mechanical properties of UMo.

An equivalent way to obtain elastic modulus is

$$\frac{1}{E_r} = \frac{1-v_1^2}{E_1} - \frac{1-v_2^2}{E_2} \quad (7)$$

where "v1" and "v2" represent poison's ratios and E1 and E2 are the elastic moduli of sample and indenter respectively. The values of poison's ratios and elastic modulus for diamond indenter are 0.07 and 1141 GPa while for the sample are 0.23 and 91GPa respectively [19, 20]. The values of H and Er are tabulated in table.1

Table: 1 Hardness and reduced elastic modulus of UMo alloy at different Mo atomic percent

Alloy	P_{max}	hc	A_c	H	Er
	nN	A^0	$x10^{-20}$ m^2	GPa	GPa
U0.71at%Mo	650.4	15.9	1747.4	37.2	93
U0.48at%Mo	338.5	17.1	1879.29	18.0	119
U0.24at%Mo	277.6	18.0	1978.2	14.0	94
U0.10at%Mo	243.1	18.7	2055.13	11.8	101

It can be seen from Fig. 4 that concentration of Mo is directly proportional to H of the material. The elastic modulus predicted by is 76 GPa and 82.9-91.5 GPa for U-10wt % Mo alloys which are found close to our findings. 10 wt% is equivalent to 0.23 at %.The small differenceisdue to geometry of the sample used together with the different order of theheat treatment [21, 22].

Doerner and Nix et.al suggested that linear fitting of the unloading data may be used to determine the stiffness, from which the hardness and modulus can be derived. We recommend that initially we have to evaluate the stiffness before the evaluation of H and Er. The evaluated slopes will be used to determine hardness and reduced elastic modulus and explanation to this step is mentioned earlier [23]. In order to fit the function at the maximum indenter's displacement, the initial process of unloading can be regarded as elastic deformation. Therefore, we choose different intervals in the unloading process for linear fitting and found out the mean value. The fitting models of unloading curves of different densities of Mo in UMo can be found from their corresponding slope by an appropriate section on the unloading curve. In the Fig. 4 (a) and (b) in the black dots are representing the fitted data obtained through simulations but in the red lines are shown the fitted curves.

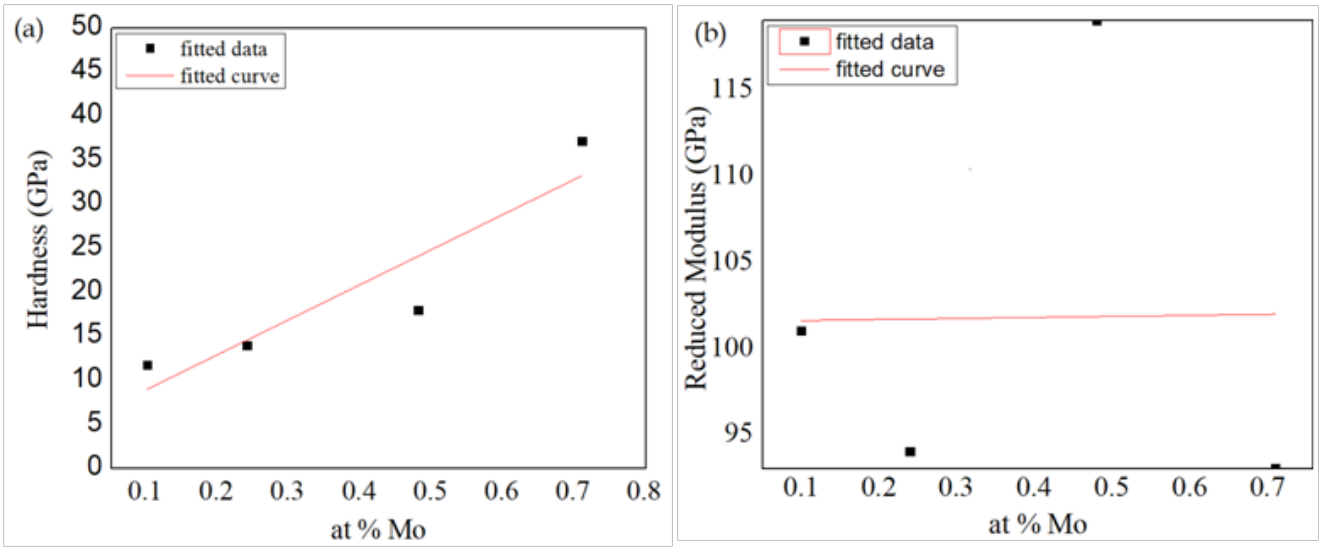

Figure 4: Hardness of the γ UMo alloys at 300 K at different concentrations of Mo From the fitted curves we can see that the hardness is directly proportional to the percent value of Mo in UMo fuel and Er is increasing but very slightly with increase in the concentration.

Conclusion

Atomistic simulations on nanoindentation was carried out using molecular dynamics simulation code LAMMPS. The U-Mo-Xe ternary EAM potential is used in this simulation. Diamond made spherical indenter investigation was carried out in order to determine the updated values for the hardness and elastic modulus of UMo fuel. Using OVITO we visualized the deformation mechanism which guided us that the atoms with the application of external forces are found in the state of motion and the area under the indenter tip is deforming while the DXA analysis confirmed that there observed no dislocations at all the said concentration of Mo. The H is increasing with increase in Mo concentration but Er is fluctuating.

Declarations

Funding: This research work was financially supported by China Scholarship Council and College of Nuclear Science and Technology, Harbin Engineering University, China. Conflicts of interest/Competing interest: No conflict of interest between the authors on the current version of manuscript.

Authors' contributions: All the authors contributed equally.

References

1. Beeler, B., Good, B., Rashkeev, S., Deo, C., Baskes, M., & Okuniewski, M. (2010). First principles calculations for defects in U. Journal of Physics: Condensed Matter, 22(50), 505703.
2. Riahi M K., Qattan I A., Hassan J., Homouz D.(2019).J. AIP. Adv. 9 055112.
3. Thyne V.,McPherson D J.(1957)Trans. Amer. Soc. Met. 49 598-619.
4. Gerard L H., Mitchell K M.,Allison E. R.(1998).Inter. Red. Enri.Reac. Conf. (22) 989.
5. Landa, A., Söderlind, P., & Turchi, P. E. A. (2011). Density-functional study of U–Mo and U–Zr alloys. Journal of Nuclear Materials, 414(2), 132-137.
6. Ewh, A., Perez, E., Keiser, D. D., & Sohn, Y. H. (2010). Microstructural characterization of U-Nb-Zr, U-Mo-Nb, and U-Mo-Ti alloys via electron microscopy. Journal of Phase Equilibria and Diffusion, 31(3), 216-222.
7. Xiao H., Long C., Tian X.,Li S.(2015).Mat. Desg.(10) 1016.
8. Fu, C. C., & Willaime, F. (2005). Ab initio study of helium in α− Fe: Dissolution, migration, and clustering with vacancies. Physical Review B, 72(6), 064117.
9. Hills R F., Butcher B R., Howlett B W.(1964).Jour. Nuc. Mat.11149-l 62.
10. Plimpton, S. (1995). Fast parallel algorithms for short-range molecular dynamics. Journal of computational physics, 117(1), 1-19.
11. Smirnova D E., Kuksin A Y., Starikov S V., Stegailov V., Insepov Z et al. (2013)Model. Sim Mat. Sci Engg. (21)035011.
12. Huang, H., Ghoniem, N. M., Wong, J. K., & Baskes, M. (1995). Molecular dynamics determination of defect energetics in beta-SiC using three representative empirical potentials. Modelling and Simulation in Materials Science and Engineering, 3(5), 615.
13. Belashchenko, D. K. (2012). Electron contribution to energy of alkali metals in the scheme of an embedded atom model. High Temperature, 50(3), 331-339.
14. Stukowski A.(2010).Model Sim Mat Sci Engg.(18) 015012.
15. Starikov, S. V., Insepov, Z., Rest, J., Kuksin, A. Y., Norman, G. E., Stegailov, V. V., & Yanilkin, A. V. (2011). Radiation-induced damage and evolution of defects in Mo. Physical Review B, 84(10), 104109.
16. Smirnova, D. E., Starikov, S. V., & Stegailov, V. V. (2011). Interatomic potential for uranium in a wide range of pressures and temperatures. Journal of Physics: Condensed Matter, 24(1), 015702.
17. Nerikar, P. V., Parfitt, D. C., Trujillo, L. C., Andersson, D. A., Unal, C., Sinnott, S. B., ... & Stanek, C. R. (2011). Segregation of xenon to dislocations and grain boundaries in uranium dioxide. Physical Review B, 84(17), 174105.
18. https://vdoc.pub/documents/nano-indentation-in-materials-science-abs6jtpko
19. Mustafa M., Qingyu W.,Zubair M.(2019).Sains. Malaysia. (48)2029–2039.
20. Amin H A.,George Z V. (2010).Acta. Mech.(209) 1–9.
21. Smirnova D E., Starikov S V.,Stegailov V.,(2012).J. Phys.: Condensed matter (24)0953-8984.
22. Nomine A., Bedere D., Miannay.(1974).Proc. 3rd Army Materials Technical Conf. (Vail, CO) (98)657–99.
23. Doerner M F.,Nix W D.,(1986). J. Mater. Res (1)987.